Torsion Balances:
An Experimenter's Handbook

M.P.Ross for the Eöt-Wash Group
University of Washington

May 27, 2022

Contents

Chapter 0

History

Chapter 1

Introduction

1.1 Simple Torsion Balance

A torsion balance, in its simplest incarnation, is an extended body, called the "pendulum," suspended from a thin wire, the "torsion fiber." This forms a rotational spring-mass system which has two intrinsic parameter (ignoring loss terms): the moment of inertia, I, and the torsional spring constant, κ. The primary degree of freedom of this system is rotation of the pendulum around the axis of the fiber which we call torsion. See Section 3.1 for discussion of other degrees of freedom.

Restricting ourselves to only the torsional degree of freedom gives us:

$$I\ddot{\theta}(t) = \sum_i \tau_i(t) \tag{1.1}$$

where θ is the angle of the pendulum about vertical, t is time, and τ_i are the torques acting on the pendulum. Here we use Newton's notation for derivatives with respect to time, $\dot{x} = \partial x/\partial t$ and $\ddot{x} = \partial^2 x/\partial t^2$.

From Hooke's law, the torsional spring adds a restoring torque that follows:

$$\tau_{\text{spring}}(t) = -\kappa(\theta(t) - \theta_0) \tag{1.2}$$

where θ_0 is the equilibrium angle of the torsion balance. For most situations this is the dominant torque acting on the pendulum.

Due to historical reasons, the classical example of a torsion balance is a dumb-bell shaped pendulum suspended from a thin metal fiber, shown in Figure 1.1. The pendulum is formed by a massless rod with two equal mass "test masses" attached to each end. The torsion fiber is then attached to the rod at equal distance to each test mass. This provides a prototypical model of a torsion balance which we will analyze in detail. Modern torsional balance apparatus typically have pendulums with more complex geometry and may have multiple suspension stages.

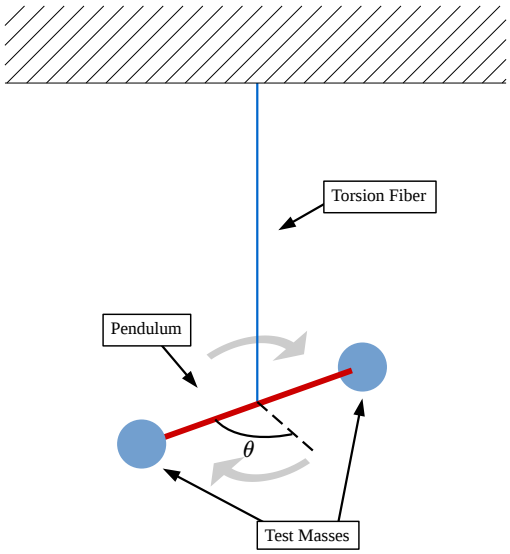

Figure 1.1: A simple torsion balance system.

1.2 Loss Terms

There are two primary sources of loss in torsion balances: external and internal damping. External damping, sometimes called velocity damping, is caused by external forces acting on the pendulum that are proportional to the angular velocity of the pendulum, such as air friction. Internal damping, on the other hand, is caused by energy dissipation internal to the torsion fiber.

External damping adds a torque on the pendulum that is proportional to the angular velocity of the pendulum:

$$\tau_{\text{vel}}(t) = -\gamma\dot{\theta}(t) \tag{1.3}$$

where γ is the damping constant. Where as internal damping can be modeled by a complex spring constant:

$$\tau_{\text{spring}}(t) = -\kappa(1 + i\delta)\big(\theta(t) - \theta_0\big) \tag{1.4}$$

where δ is the dimensionless internal loss parameter.

For most modern torsion balances, external damping is engineered away and is thus much smaller than the internal damping. Thus we will shelve discussion of external damping until Section 4.7

1.3 Equations of Motion

As mentioned in Section 1.1, the simple torsion balance is described with two primary parameters: the moment of inertia, I, which is determined by the pendulum geometry, and the torsional spring constant, κ, which is determined by the torsion fiber size and material. Adding in internal damping, this system obeys the following equation of motion:

$$I\ \ddot{\theta}(t) + \kappa(1 + i\delta)\big(\theta(t) - \theta_0\big) = \tau_{\text{ext}}(t) \tag{1.5}$$

where $\tau_{\text{ext}}(t)$ is the sum of all exterior torques acting on the pendulum.

If we assume a harmonic solution, $\theta(t) = A\ e^{i\omega t}$, we can transform Equation 1.5 into the Fourier domain to yield:

$$\big(-I\omega^2 + \kappa(1 + i\delta)\big)\tilde{\theta}(\omega) = \tau_{\text{ext}}(\omega) \tag{1.6}$$

It is convenient to define two parameters here: the resonant frequency, $\omega_0 = \sqrt{\kappa/I}$, and the quality factor, $Q = \frac{1}{\delta}$. Equation 1.6 can then be rearranged to:

$$\tilde{\theta}(\omega) = \frac{\tau_{\text{ext}}(\omega)}{\kappa} \frac{1}{1 - \omega^2/\omega_0^2 + i/Q} \tag{1.7}$$

1.4 Response Function

The second dimensionless factor in Equation 1.7 is traditionally called the response function or transfer function of the system. It controls the amount of angle the pendulum gets for a given torque as a function of frequency.

$$\Lambda(\omega) = \frac{1}{1 - \omega^2/\omega_0^2 + i/Q} \tag{1.8}$$

For a pendulum with no damping, $Q \to \infty$, the response function has three distinct features. Below the resonant frequency, $\omega << \omega_0$, the response goes to unity. Above the resonant frequency, $\omega >> \omega_0$, the response function follows $\Lambda(\omega) = -\omega_0^2/\omega^2$ causing effect of high frequency torques to decrease as $1/\omega^2$. At the resonant frequency, $\omega = \omega_0$ the response goes to infinity. This causes the motion at this frequency to grow without limit.

With damping, the response has a similar structure albeit with different amplitudes. Namely at the resonance the response does not approach infinity but instead $\Lambda(\omega) = -iQ$. The quality factor, hence the amount of damping, limits the maximum resonant motion for a given input torque.

The full response function is plotted in Figure 1.2 for a variety of quality factors and a resonant frequency of 0.1 Hz. As can be seen, below the resonance the magnitude of the response approaches unity with a nearly zero phase for most values of Q. There's a peak at the resonant frequency whose amplitude is strongly dependent on Q and the phase undergoes a rapid transition. Above the resonance the magnitude follows $\sim 1/\omega^2$ with a phase of 180° independent of Q-value. Note that a phase of 180° is equivalent to a negative sign.

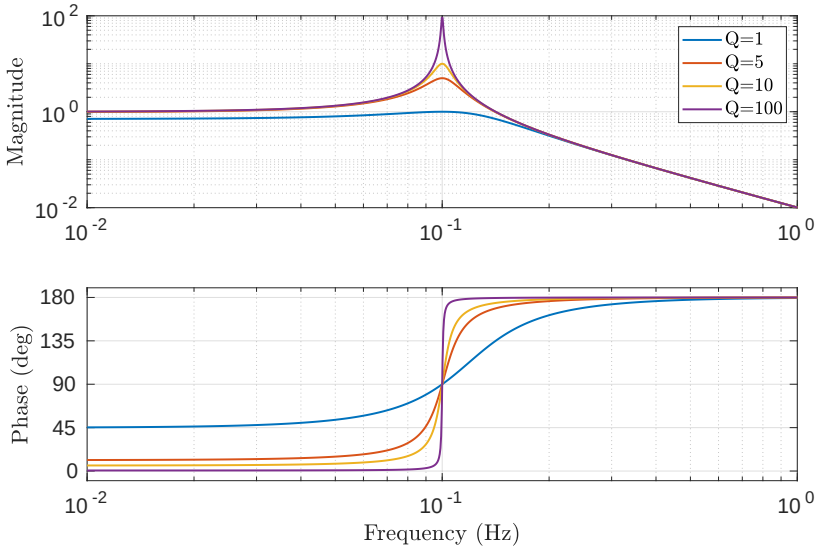

Figure 1.2: The response function for a simple torsion balance system with a resonance of $\omega_0 = 2\pi$ (0.1 Hz).

Chapter 2

Mechanics

2.1 Torque Sensing

For many experiments, the primary use of a torsion balance is to sense weak torques acting on the pendulum. In this mode, the measurements of the angle of the pendulum is converted to torque by rearranging Equation 1.7:

$$\tau_{\text{ext}}(\omega) = \frac{\kappa\ \tilde{\theta}(\omega)}{\Lambda(\omega)} \tag{2.1}$$

If we assume a frequency-independent angle spectrum, $\tilde{\theta}(\omega)$, (which is unrealistic but a rough approximation of spectra arising from readout noise, Section 4.2) then the corresponding torque spectrum will follow the inverse of the pendulum response function, $\Lambda(\omega)$. An example of such a spectrum is shown in Figure 2.1. This spectrum has very similar features as the response discussed in Section 1.4. However, instead of having a peak at the resonant frequency it has a dip and above the resonant frequency the torque spectrum rises as $\sim \omega^2$.

These features are the first example we've seen that expresses the significance of the frequency of signal of interest in designing an experiment. A careful experimenter would design an apparatus to minimize the noise at the frequency of interest within practical limits. For example, the model apparatus described by Figure 2.1 would not be ideal to run an experiment with a signal at 1 Hz but would be well suited for a signal at 10 mHz since the noise level differs by a factor of 100 between these two frequencies. This is a common consideration in torsion balance design that will reoccur throughout this work.

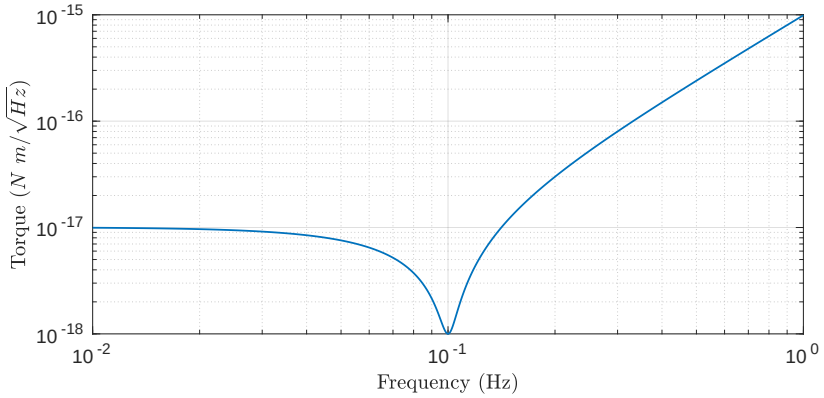

Figure 2.1: Example torque spectrum assuming a frequency independent angle spectrum $\tilde{\theta}(\omega) = 1$ nrad/$\sqrt{\text{Hz}}$ amplitude, $\kappa = 10^{-8}$ N m/rad, $Q = 10$, and $\omega_0 = 2\pi$ (0.1 Hz) .

2.2 Inertial Sensing

A relatively newer use of torsion balances is for inertial sensing. Where as in the previous section we discussed torques acting on the pendulum, for inertial sensing the pendulum acts as an inertial proof mass. The goal of this mode is to measure the angular motion of structure that the pendulum is suspended from. These sorts of measurements have a wide range of application, from rotational seismology and seismic isolation to guidance systems and navigation.

A system whose support structure is allowed to move can be modeled with Equation 1.5 by allowing θ_0 to vary in time:

$$I\ \ddot{\theta}(t) + \kappa(1 + i\delta)\big(\theta(t) - \theta_0(t)\big) = \tau_{\text{ext}}(t) \tag{2.2}$$

Since the motion of the support is what we want to measure, Equation 2.15 can be transformed in the Fourier domain and rearranged to yield:

$$\tilde{\theta}(\omega) = \frac{1 + i/Q}{1 - \omega^2/\omega_0^2 + i/Q}\ \tilde{\theta_0}(\omega) \tag{2.3}$$

However, angular readout systems do not sense the inertial angle of the pendulum but instead measure the difference in angle between the support and the pendulum. (In all other sections we assume the support is inertial.) Thus, the measured angle is:

$$\tilde{\theta_a}(\omega) = \tilde{\theta}(\omega) - \tilde{\theta_0}(\omega) \tag{2.4}$$

Combining Equations 2.3 and 2.4 yields:

$$\tilde{\theta_0}(\omega) = \frac{\omega_0^2}{\omega^2}\ \frac{1}{\Lambda(\omega)}\ \tilde{\theta}_a(\omega) \tag{2.5}$$

At first glance, Equation 2.5 looks very similar to the angle response to torque, Equation 1.7. However, the extra factor of ω^2/ω_0^2 mirrors the features onto opposite sides of the resonance. For a frequency independent measured angle spectrum, the inertial angle spectrum will follow $\sim 1/\omega^2$ below the resonance while above it flattens to approach the measured angle spectrum. Figure 2.2 shows an example of such a spectrum which displays the same features as Figure 2.1 but mirrored about the resonance frequency.

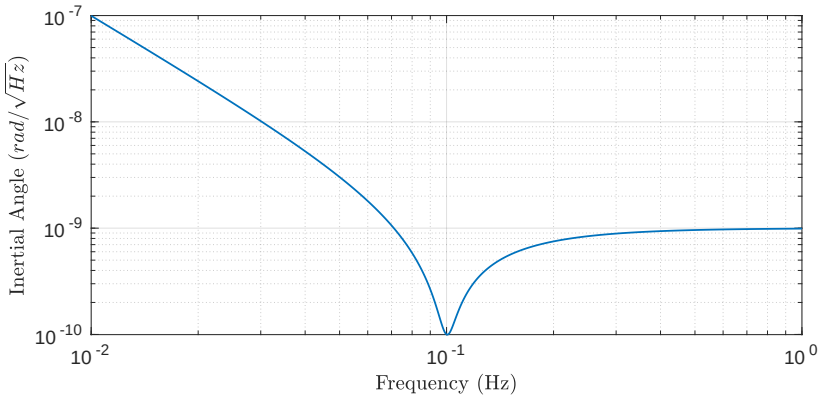

Figure 2.2: Example inertial angle spectrum assuming a frequency independent measured angle spectrum $\tilde{\theta_a}(\omega) = 1$ nrad/$\sqrt{\text{Hz}}$ amplitude, $Q = 10$, and $\omega_0 = 2\pi$ (0.1 Hz).

Due to the features of Equation 2.5, an inertial sensing apparatus achieves its best performance above the resonant frequency and quickly looses sensitively below it. Thus lowering the resonant frequency increases the band of interest.

2.3 Fiber Engineering

Although it is easy to think of the torsion fiber as a minor part of the torsion balance system, manufacturing the optimal fiber for a given experiment is an art in itself. There are two primary optimizations when designing a torsion fiber: minimizing the κ of the fiber and maximizing the Q. These are not necessarily orthogonal and many design alterations will drastically change both parameters.

There is generally three parameters that can be adjusted in a fiber design: the length of the fiber, l, the cross-sectional radius[1], r, and the material. To optimize these parameters, one usually uses the following procedure. First, find out the maximum length that can fit in the given apparatus and use that length of fiber. Then choose a material based on the requirements of the experiment, what is readily available to purchase or manufacture, and which material will

[1]Here we're assuming a circular cross-section but many fibers have more complex geometries which must be accounted for.

give the highest Q. Then minimize the fiber radius until the weight of the pendulum is close to the breaking strength of the fiber (with a healthy safety factor to minimize break-ability). This can be iterated through multiple times along with various apparatus changes (chamber height, charge mitigation, etc.) to achieve a near optimal set-up.

Experimenter's are not left to blindly search for optimal parameters but are instead informed by vast troves of theoretical and experimental information much of which was produced by the engineering communities. The κ-value for a fiber with uniform cross-section can be readily calculated using [1]:

$$\kappa = \mu \frac{J}{l} \tag{2.6}$$

where μ is the shear modulus of the material, J is the torsional constant of the material, and l is the length of the fiber. The shear modulus depends on the material and temperature whereas the torsional constant only depends on the cross-sectional geometry of the fiber. Assuming a circular cross-section this becomes:

$$\kappa = \mu \frac{\pi r^4}{2l} \tag{2.7}$$

where r is the cross-sectional radius of the fiber. Equation 2.7 shows the drastic dependence of κ on the radius of the fiber and to a lesser extent the length. The value of the shear modulus, μ, for a given material is typically looked-up in various engineering references. Table 2.1 gives the values for a selection of materials typically used in torsion balance apparatus.

Material	Shear Modulus, μ (GPa)
Beryllium Copper (Be-Cu)	48
Aluminum (Al), 6061-T6	224
Tungsten (W)	161
Titanium (Ti)	41
Steel	75
Fused Silica (SiO_2)	31

Table 2.1: Table of the shear modulus for a selection of typical materials [2, 3].

Naively, Equation 2.7 could be interpreted as allowing arbitrarily low κ-values since up to this point we have not set any limits on the minimum width of the torsion fiber. However, in addition to providing the restoring torque, the fiber must also hold the pendulum's weight. The maximum force that a fiber

can experience without deforming[2] follows:

$$F = \sigma \pi r^2 \tag{2.8}$$

where σ is the yield strength of the material and r is the cross-sectional radius. The minimum radius needed to hold a pendulum is then:

$$r_{\text{min}} = \sqrt{\frac{mg}{\pi \sigma}} \tag{2.9}$$

where m is the mass of the pendulum and g is the local gravitational acceleration. A fiber of this radius could hold the pendulum but any further force (Earthquake, anthropogenic forces, etc.) on the fiber would cause it to yield. Thus a safety factor is used to ensure the apparatus is robust against laboratory conditions.

$$r_{\text{safe}} = \eta \sqrt{\frac{mg}{\pi \sigma}} \tag{2.10}$$

where η is the safety factor with typical values in the range of 2 - 3. Yield strength is another parameter which in practice is looked-up in engineering references. Table 2.2 shows values for a collection of typical materials used for torsion fibers.

Material	Yield Strength, σ (MPa)
Beryllium Copper (Be-Cu)	965 - 1205
Aluminum (Al), 6061-T6	241
Tungsten (W)	550
Titanium (Ti)	100 - 225
Steel	75
Fused Silica (SiO_2)	48

Table 2.2: Table of yield strengths for a selection of typical materials [3, 4, 5, 6].

The quality factor, Q, is also an important consideration when engineering a torsion fiber. The Q-value is inversely proportional to the amount of mechanical energy dissipated in the fiber. Thus, the Q-value not only changes the response function of the system, as can be seen in Figure 1.2, but also influences the amount of thermal noise in the system. Thermal noise is discussed in detail in

[2]There are two tensile strengths one could use: the yield strength or the ultimate tensile strength. The yield strength is the point at which the material deforms while the ultimate tensile strength is when it breaks. The ultimate tensile strength is typically less than twice the yield strength. Here we use the yield strength as it is lower than the ultimate tensile strength and deformation of a torsion fiber would alter the other parameters discussed here.

Section 4.1; however when it comes to fiber design the important fact is that thermal torque noise follows, $\tau \sim 1/\sqrt{Q}$. Thus the higher the Q the lower the thermal noise.

The exact value of the quality factor of a given fiber is dependent on a variety of factors, from the mechanics of the end points to the presence of surface defects. However, many materials are known to have larger Q-values than others. Generally, if the material is more uniform then it will have a larger Q-value. Metals are the traditional choice especially those historically used in musical instruments (bells, guitar strings, etc.). Specifically, tungsten fibers are known to achieve Q-values of $\sim$ 4500 [7]. A type of glass called fused silica or fused quartz is also well known to be a high-Q material. It is formed from almost pure silicon dioxide (SiO_2) and can achieve Q-values as high as 10^5 [7]. As compared to metals, fused silica is extremely delicate and thus many hours of lab work can be ruined by simply touching the fiber. To many experimenter's, including those at the world's gravitational wave observatories, this risk is well worth the exceedingly high Q-values achieved by this material.

2.4 Pendulum Design

Engineering a suitable fiber doesn't in itself make for a high-quality torsion balance; a quality pendulum is the other key ingredient. Much of the pendulum design depends strongly on the experiment that is to be conducted with the apparatus. Yet there are a few common guidelines that lead to the top performing pendulums.

With every pendulum, there is mass that is used in the scientific experiment, which we call active mass, and mass that only serves as structural support, called passive mass. In the simple torsion pendulum shown in Figure 1.1, the active mass would be the test-masses while the passive would be the rod. Since many experiments are more sensitive if the apparatus has more active mass, experimenter's want to maximize the active mass and minimize the passive. The figure of merit for a given pendulum design is the ratio of the active mass and the total mass:

$$\alpha = \frac{m_{\text{active}}}{m_{\text{active}} + m_{\text{passive}}} \tag{2.11}$$

Ideally, $\alpha = 1$ (such as in the massless-rod, simple pendulum example) which would imply that all of the mass of the pendulum is participating in the experiment. However, no realistic pendulum achieves this and α-values of 40-60% are considered satisfactory.

The other parameter that is directly controlled by the pendulum design is the moment of inertia, I. The moment of inertia can be calculated via:

$$I = \int \rho(\vec{r})\ r^2\ dV \tag{2.12}$$

where $\vec{r}$ is the vector from the rotation axis to a point in the pendulum, ρ is the mass density at that point, and dV is the corresponding volume element. This

integral is taken over the entire volume of the pendulum. If we align the z-axis with the torsion fiber then the torsional moment inertia[3] can be found with:

$$I = \int \rho(x, y, z)\ (x^2 + y^2)\ dx\ dy\ dz \tag{2.13}$$

For the simple torsion balance described in Section 1.1 the mass density is simply Dirac delta functions which follow (aligning the x-axis with the pendulum rod):

$$\rho(x, y, z) = m\ \delta(x^2 - R^2)\ \delta(y)\ \delta(z) \tag{2.14}$$

where m is the mass of one test mass and R is the "lever-arm" (the radius from the torsion fiber to the test masses). The moment of inertia then simplifies to:

$$I = 2mR^2 \tag{2.15}$$

Although Equation 2.15 is for an idealized pendulum, moments of inertia for realistic geometries follow the same scaling (i.e. $I \sim mR^2$). The primary effect of the moment of inertia on the equation of motion is the change of the resonant frequency:

$$\omega_0 = \sqrt{\frac{\kappa}{I}} \sim \frac{1}{R}\sqrt{\frac{\kappa}{m}} \tag{2.16}$$

The lever-arm not only affects the moment of inertia but can also influence the sensitivity of a given experiment. If the experiment is searching for a new force, $\vec{F}_{\text{new}}$, then the torque experienced by the pendulum will follow:

$$\tau(t) = \vec{r} \times \vec{F}_{\text{new}} \sim R\ F_{\text{new}} \tag{2.17}$$

Thus for a given torque sensitivity, the larger the lever-arm the more sensitive the experiment is to new forces. This is why most experimenters place the test masses at the largest radius allowed in the given apparatus.

In addition to maximizing the active mass and tuning the geometry, a pendulum design must account for a variety of extraneous couplings and noise sources that are addressed in later sections. These include allowing angle readout, Section 4.2, minimizing electrostatic coupling, Section 4.4, and accounting for gravity gradients, Section 4.8.

[3]There is a different moment of inertia for each rotation axis. Here we only calculate the torsional moment (i.e. for rotations around the z-axis) but a similar procedure can yield the other moments. Generally, there's a moment of inertia tensor which allows one to calculate the moment around any axis of rotation.

Chapter 3

Complications

3.1 Swing Modes

Up to this point, we have only focused on the torsional degree of freedom but any torsion balance with a non-zero length torsion fiber will also permit "swing" modes. These are the prototypical pendulum modes whose restoring force is due to gravity not the torsion spring. Figure 3.1 shows the swing degree of freedom for our simple torsion balance system.

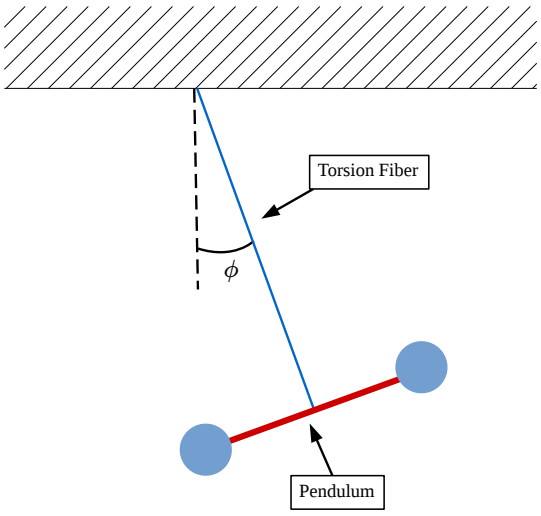

Figure 3.1: The swing degree of freedom for a simple torsion balance system.

Restricting ourselves to one swing axis and allowing for external damping of

this motion, the equation of motion for the swing degree of freedom is:

$$I_\phi \ \ddot{\phi}(t) + \gamma_\phi \dot{\phi}(t) - \tau_g(t) = \tau_\phi(t) \tag{3.1}$$

where I_ϕ is the moment of inertia about the swing axis (into the page in Figure 3.1), ϕ is the swing angle of the pendulum, γ_ϕ is the swing damping constant, τ_g is the gravitational restoring torque, and τ_ϕ is the exterior torque about the swing axis. Treating the pendulum as a point mass gives:

$$ml^2\ddot{\phi}(t) + \gamma_\phi \dot{\phi}(t) + mgl\sin(\phi(t)) = \tau_\phi(t) \tag{3.2}$$

where m is the mass of the pendulum, l is the length of the torsion fiber, and g is the local gravitational acceleration. If we take the small-ϕ approximation the equation of motion becomes:

$$\ddot{\phi}(t) + \frac{\gamma_\phi}{ml^2}\dot{\phi}(t) + \frac{g}{l}\phi(t) = \frac{\tau_\phi(t)}{ml^2} \tag{3.3}$$

If we define $\nu_0 = \sqrt{g/l}$ and $\nu_0/\Omega = \gamma_\phi/(ml^2)$, the equation of motion in the Fourier domain becomes:

$$\phi(\omega) = \frac{\tau_\phi(t)}{mgl}\frac{1}{1-\omega^2/\nu_0^2 + i\omega/(\nu_0\Omega)} \tag{3.4}$$

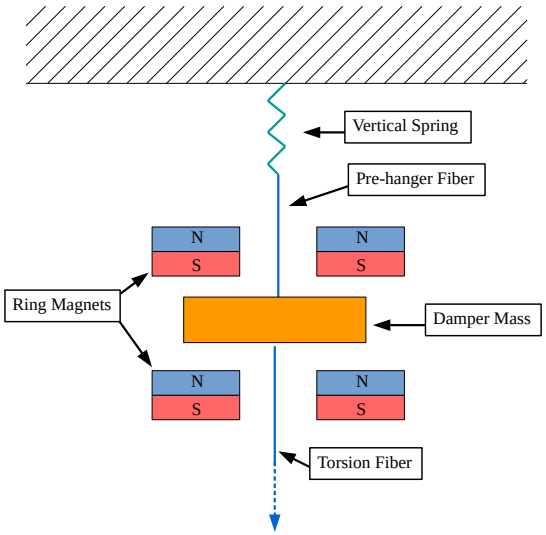

Figure 3.2: Schematic of eddy-current damper.

Excess swing motion can have detrimental effects on the performance of an apparatus. The primary effect of swing motion is addition noise in the

torsional degree of freedom. This can be caused by either mechanical cross-coupling converting swing motion into torsional motion or, more commonly, non-linearities in the angular readout systems, Section 4.2, causing swing to register as torsional readings. Thus, any sensitive torsion balance will include some method to limit this swing motion.

The traditional way to limit swing motion is with the addition of an eddy-current swing damper, shown in Figure 3.2. This consists of a conducting damper-mass which is suspended from a pre-hanger fiber and a vertical spring. The torsion balance is then suspended from the damper-mass. The pre-hanger fiber is typically larger diameter than the torsion fiber to separate the double pendulum modes. To achieve eddy-current damping this mass is placed is a non-uniform magnetic field typically produced by a pair of ring magnetics held by an independent structure.

As the damper mass moves in the non-uniform magnetic field, eddy currents are produced in the mass which dissipates the mechanical motion.

3.2 Centrifugal Force

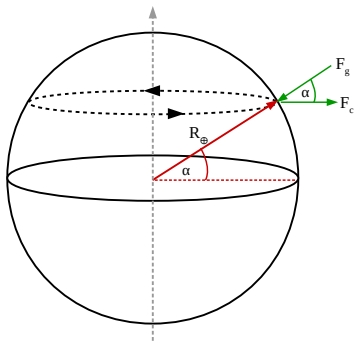

Figure 3.3: Geometry of forces caused by having the torsion balance on the surface of the Earth.

For most practical purposes, we assume that the torsion fiber runs parallel to local gravity. If the Earth was a perfect sphere the fiber would point directly towards the center of the Earth. However, this is only true if the torsion balance is located at either the equator or one of the planet's poles. Torsion balances experience two forces due to being located on the surface of the Earth: the gravitational pull of the Earth and the centrifugal force due to the Earth's rotation. These together determine the equilibrium swing angle which is not pointed along local gravity.

Since the Earth is rotating, the torsion balance feels a centrifugal force that

points perpendicular to the rotation axis of the Earth and follows:

$$F_c = m\omega_\oplus^2 R_\oplus \cos\alpha \tag{3.5}$$

where m is the mass of the pendulum, $\omega_\oplus$ is the angular frequency of the Earth, $R_\oplus$ is the radius of the Earth, and α is the latitude of the torsion balance's location. Figure 3.3 shows the geometry of this force along with the gravitational force due to the Earth.

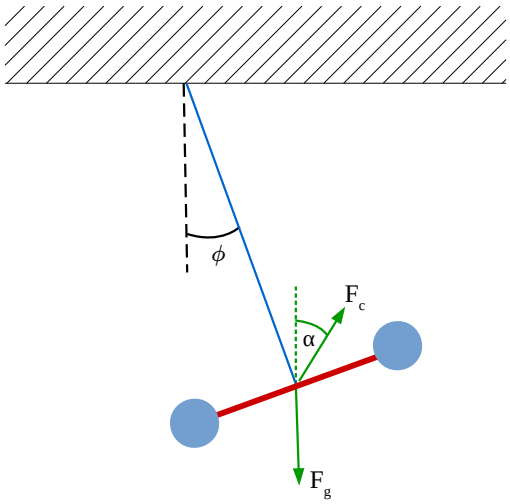

Figure 3.4: Force diagram for the forces acting on the torsion balance in equilibrium.

In the lab frame, the centrifugal force points upwards at an angle from local vertical equal to the latitude of the torsion balances location as shown in Figure 3.4. This provides an additional torque on the balance which shifts its swing equilibrium angle to be:

$$\phi_0 = \arctan\left(\frac{\omega_\oplus^2 R_\oplus \cos\alpha \sin\alpha}{g - \omega^2 R_\oplus \cos^2\alpha}\right) \tag{3.6}$$

Figure 3.5 shows the Equation 3.6 evaluated at a collection of northern hemisphere latitudes. The southern hemisphere (negative latitudes) has the same magnitude effect but opposite sign. This effect is maximum at 45° latitude at which the pendulum hangs ~ 1.7 mrad away from local vertical.

Although this shift has little effect on many experiments, it allows torsion balances to use the Earth as a source mass at most latitudes. This is used in many equivalence principle tests as well as using torsion balances for geophysical exploration.

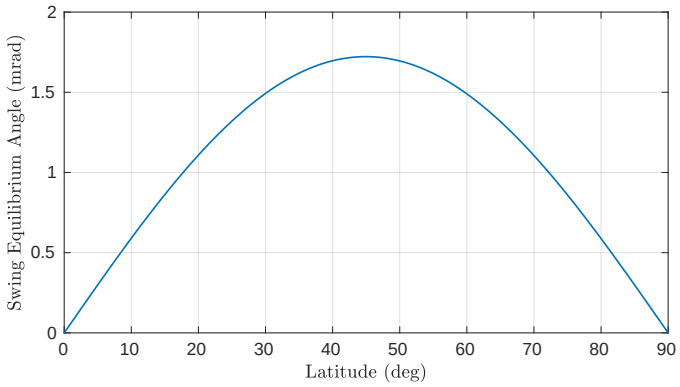

Figure 3.5: Plot of swing equilibrium angle vs. latitude.

Chapter 4

Noise Sources and Mitigation

Although experimenters try their hardest, torsion pendulums do not exist in the pristine environments we like to cook up on chalkboards. The have a long list of interactions with the universe that end up plaguing experiments. Calling an effect noise verses signal is a choice of viewpoint. Here we will assume the science being conducted is not related to the environment but is instead a novel force or a torque that's controlled by the experimenter. Of course noise can become signal if one was aiming to study one of these effects.

4.1 Thermal Noise

The fact that torsion balances are at finite temperature causes ever-present "thermal" noise which is one of the most difficult to mitigate. There are multiple ways to view this noise source. On a microscopic level, it is caused by the thermal motion of the atoms that make up the torsion fiber. Abstracting a bit more, it is due to application of the fluctuation-dissipation theorem [8] to the torsion balance system.

This thermal motion causes a stochastic torque that follows [9]:

$$\tau(\omega) = \sqrt{4k_B T\left(\frac{\kappa}{Q}\right)\left(\frac{1}{\omega}\right)} \tag{4.1}$$

where k_B is Boltzman's constant, T is the temperature, κ is the spring constant, Q is the quality factor, and ω is the angular frequency. Note that this torque noise follows $\sim 1/\sqrt{\omega}$ and thus increases in amplitude at lower frequencies. An example thermal noise is plotted in Figure 4.1 along with an example readout noise, Section 4.2.

There are three parameters that can be altered to minimize this noise. For most torsion balances the temperature is set by the ambient temperature of

the laboratory; however, a few experimenter's have investigated cooling their apparatus to cryogenic temperatures. The other two, κ and Q, are determined by the torsion fiber and thus readily engineered.

We've already seen that minimizing the κ-value increases a torsion balance's sensitivity to torques but Equation 4.1 shows an additional benefit of lowering the amplitude of thermal noise. Additionally, maximizing the Q-value further decreases the amplitude. Although these techniques can decrease the influence of this noise on a given apparatus, thermal noise can never be completely avoided and limits the performance of many torsion balance apparatus.

4.2 Readout Noise

The angle of the torsion balance needs to be measured in someway. In today's world, this is done almost exclusively with some sort of analog, precision measuring device communicating to a computer through a analog-to-digital converter (ADC). The measuring device can either directly measure the change in angle (autocollimator, optical levers, etc.) or measure the translation of a part of the pendulum (interferometers, capacitors, etc.).

If the device's native units are translation, then the measurements must be translated into angle using the following:

$$\sin\big(\theta(t)\big) \approx \theta(t) = \frac{x(t)}{a} \tag{4.2}$$

where $x(t)$ is the recorded translation and a is distance from the torsion fiber axis to the measurement point. In order to maximize the sensitivity of the experiment, astute experimenters who deploy such readout schemes place the measurement point as close to the edge of the pendulum as possible[1], $a \approx R$.

The act of turning the analog angle measurement to a digital signal that computers can handle causes a noise called "quantization" noise. Analog signals are continuous but digital signals are quantized. To map an analog reading to a quantized digital signal, the ADC rounds the analog reading to the closest digital output allowed by the device. ADCs are built with a select number of allowed digital outputs depending on the number of bits that the ADC has and its voltage range. There are 2^n numbers that can be represented with n bits. An ADC with 2 bits (4 values) and a voltage range of 0-6 V can only output the values 0,2,4,6. Commonly ADCs come in 8-bit (256 values), 16-bit (65,536 values), and 24-bit (16,777,216 values).

The rounding of the analog signal to one of the allowed ADC values can turn small fluctuation of the analog signal into large jumps between two ADC values, i.e. quantization noise. For example in our 2-bit ADC example, if the analog signal is exactly 3 V then the ADC would round up and output at 4. But if the 3 V fluctuated down by 1 μV (from thermal effects in the circuit, ambient electromagnetic waves, etc.) then the ADC would round down to 2. Run this over a period of time and the ADC would record a series of 4s and 2s

[1] Yet another place where large lever-arm helps the experiment.

with equal number of the two. This switching between ADC states is the cause of quantization noise.

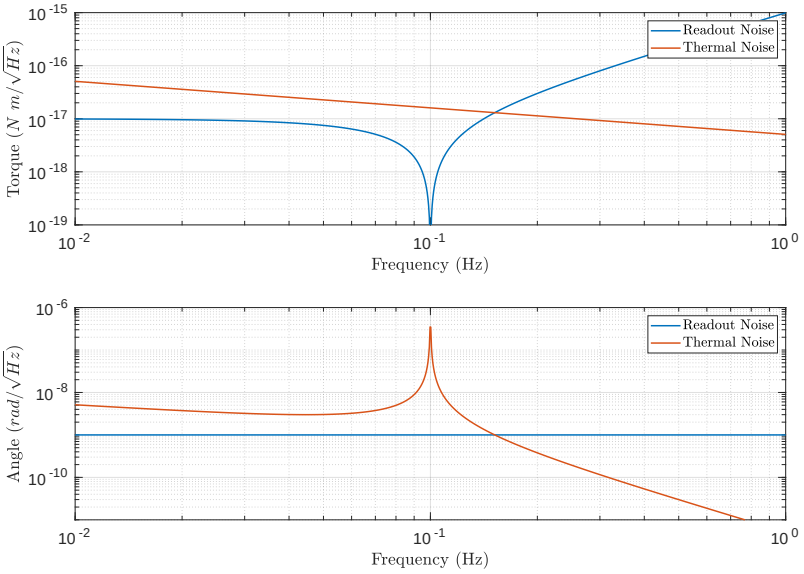

Figure 4.1: Example torque-noise and equivalent angle-noise spectra assuming a readout angle spectrum of $\tilde{\theta}(\omega) = 1$ nrad/$\sqrt{\text{Hz}}$ amplitude, $\kappa = 10^{-8}$ N m/rad, $Q = 10^6$, $T = 293$ K, and $\omega_0 = 2\pi$ (0.1 Hz). The total observed noise of such a system would be the sum of the two contributions.

The exact level of the ADC noise depends of the details of the system but roughly follows:

$$n_{\text{quant}} \propto \frac{V_{\text{range}}}{2^n} \frac{1}{\sqrt{f_{\text{samp}}}} \tag{4.3}$$

where n_{quant} is the noise level, V_{range} is the voltage range of the ADC, n is the number of ADC bits, and f_{samp} is the sampling frequency. Thus there are typically two paths to decrease the quantization noise of an instrument. The most straight forward way to to increase the bits of the ADC which makes the gaps between ADC numbers smaller. This tends to be limited by what ADCs are available on the market. The other way is to record at a faster sample rate. The faster data rate can allow the signal to be averaged to a lower rate, higher precision signal. The noise in this averaged signal decreases as the square root of the number of samples (faster rate equals more samples). This is also limited by the ADC on the market as they tend to have a maximum rate that they can be ran. But this can also depend of the rate of the downstream data pipeline. If the program used to record the data can't run as fast as the ADC then the

program will be the limiter on the data rate.

Quantization noise typically has a "white" spectrum (i.e. same value at all frequencies) that can limit the sensitivity of a readout if it has no other noise sources. This can be seen in Figure 4.1 which shows this readout noise along side an example thermal noise, Section 4.1. Notice that the readout noise is flat in angle units since that's the native units of the measurement but when converted to torque, the readout noise rises at high frequencies. The combination of the readout noise and thermal noise give many apparatus a bucket shaped torque noise sensitivity. In such systems, the highest sensitivity is when the two noise sources cross over. As such, experimenters can alter the parameters of the apparatus to place this minimum at the frequency of interest.

Many realistic readouts are not only limited by quantization noise but also have noise caused by harder-to-model sources (electronics, sustainability to temperature changes, etc.). These can make a readout have a more complicated spectral shape. A common shape is a "pink" noise spectrum which follows $1/\sqrt{f}$ or $1/f$. Since these spectra are nearly flat, they also form a sensitivity bucket albeit with a steeper edge. Decreasing this sort of readout noise is more specific to the exact readout system but can range from using low-noise electronics and controlling or insulating from temperature changes to minimizing air currents and patch charges.

4.3 Seismic Motion

Even though we don't perceive it in our everyday lives, the ground is always moving. Whether from human activity, the oceans, or the atmosphere, ground motion is constantly being driven. This can be seen in Figure 4.2 which displays the amplitude spectral density of typical horizontal seismometer readings [10]. Seismometers are spring-mass systems that use the same dynamics as those described in Section 2.2 to measure ground motion above their resonant frequency.

Different sources cause motion at distinct frequencies. Above 1 Hz the motion is typically dominated by anthropogenic sources. Whether it's fans from equipment and heating system or vibrations from cars, buses, and trains, human activity causes significant ground motion. This motion typically only appears above 1 Hz due the time scales of most human activity and the dominance of the oceanic microseism at lower frequencies.

There are persistent, long-wavelength pressure waves within the ocean's water column that are caused by the interference between atmospherically driven surface waves and the ocean floor. These pressure waves drive the dominant persistent ground motion seen everywhere on Earth which we called the oceanic microseism (or just microseism for short). The exact amplitude and frequency content of this motion depends on oceanic weather but every seismometer on the surface of the Earth senses a broad peak typically between 10 mHz - 1 Hz with peak amplitude of 0.1 - 1 μm/s/$\sqrt{\text{Hz}}$. At frequencies lower than $\sim$10 mHz, true ground motion is relatively low but seismometer readings become dominated by

ground rotations. See Reference [10] for more details on ground rotations.

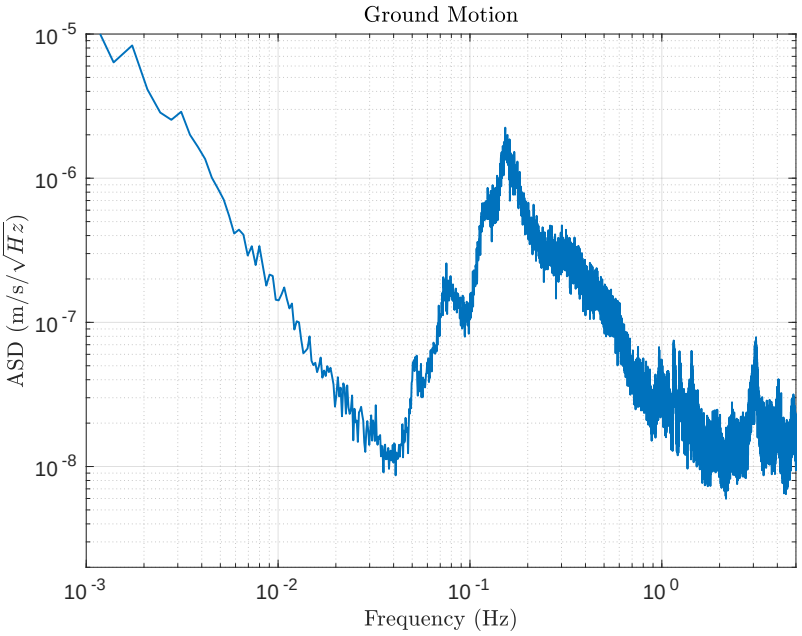

Figure 4.2: Amplitude spectral density of typical ground motion as recorded by a horizontal seismometer. [10] The spectrum is dominated by anthropengic motion above 1 Hz and the microseism between 30 mHz - 1 Hz. Below 30 mHz the spectrum is dominated by ground rotations caused by the atmosphere.

In addition to the persistent ground motion, there are many sources of large, short-duration motion. The most obvious case is Earthquakes but humans also cause such transient with construction activity, explosions (both for mining and weapons testing), etc. The motion caused by these events can be much larger than the spectrum shown in Figure 4.2. However, since these events are transient, many experiments are just paused until the motion stops. As long as the apparatus is not damaged than this only amounts to a loss of data taking time which is acceptable in many circumstances.

The source of ground motion is not necessarily important for torsion balance experiments however, the apparatus must be isolated from this motion in order to achieve high sensitivity. Without isolation, ground motion would swamp any measurement and in many cases make the apparatus not function at all. There are a many methods to isolate from this motion but they broadly fit into two categories: active isolation and passive isolation.

Active isolation is the process of sensing either the ground motion or the motion of the apparatus and counteracting these motions with some sort of actuator. A system which senses ground motion is called a “feed-forward” system

because the apparatus is moved based on what is expected to happen, whereas sensing the apparatus motion is called a "feed-back" system because the applied motion is based on what has already happened. The exact development of active isolation system falls under the study of control system which has an extensive history and literature from a wide range of fields. Typically these active systems can perform superbly but are limited by the quality of sensors and actuators that are deployed and cost a large sum of both money and development time.

Passive isolation systems on the other hand tend to be simple in their design. A passive system uses the dynamics of mechanical systems to isolate from motion. Classical examples of these systems are placing the apparatus on rubber or springs and hanging the apparatus from a pendulum. This causes the apparatus to become a oscillator system which has a response function like those shown in Figure 1.2. Above the resonant frequency of the system, the motion of the apparatus is decreased by a factor of $\sim (\omega_0/\omega)^2$ where ω_0 is the resonant frequency of the system and ω is the frequency of motion. If multiple passive systems are stacked than the motion is decreased by $\sim (\omega_0/\omega)^{2N}$ where N is the number of systems.

Torsion balances are inherently passive isolation systems. The dynamics of the swing degree of freedom, Section 3.1, passively isolated the pendulum from horizontal motion. With the addition of a vertical spring at the suspension point, experimenters can also passively isolate from vertical motion. Historically, the combination of the inherent horizontal isolation and a vertical spring achieved sufficient isolation to make seismic motion subdominant except during abnormal conditions (Earthquakes, construction nearby, etc.).

Many extremely sensitivity apparatus today are employing multiple layers of both active and passive seismic isolation. For example, the LIGO gravitational wave observatories deploy three layers of active isolation and four layers of passive in the form of a quadruple pendulum. How much and which types of isolation is up to the experimenter to decide while designing an apparatus based on the frequency of interest and the necessary sensitivity of the instrument.

4.4 Electrostatic Couplings

The electromagnetic force is 10^{40} times stronger than gravity. Since many torsion balance experiments are aimed at measuring gravity or forces weaker than gravity, electromagnetic interactions can easily swamp the interactions of interest. The primary method of eliminating these interactions is to ensure that the pendulum and the surrounding structure does not collect charge.

Whether from cosmic rays or interactions with residual gas, charges will naturally collect on every surface. The goal of the experimenter is to give these charges a path to flow to ground.[2] Thus an ideal experiment would be

[2]Both positive and negative net charges can be imparted on the pendulum. Realistically, only with excess electrons on the pendulum (negative charge) would charges flow to ground. With positive net charge, electrons flow from ground to the pendulum but this can be viewed as the flow of a deficit of electrons to ground.

made solely of perfect conductors which are connected to ground. This way any momentarily charge build up would flow quickly to ground leaving the apparatus with negligible effect.

Unfortunately, short of making the apparatus out of pure superconductors (an immensely difficult task), real world experimenters don't have access to perfect conductors. Most metals are good conductors (low resistivity) yet have a non-zero resistivity. Table 4.1 shows the resistivity for a collection of common pendulum materials. This causes imparted charges to flow to ground more slowly than a perfect conductor would allow. For most applications, this slow down of charge flow is much too fast to effect the apparatus.

The more insidious effect with most metals is that they are not chemically inert. Many common metals readily interact with the oxygen in the atmosphere and water to form oxides. This is why the Statue of Liberty is green and why iron turns to rust. Pieces built for scientific apparatus are typically machined shortly before they enter use. Yet oxide layers form on the exterior these piece almost instantaneously upon exposure to the atmosphere. As can be seen in Table 4.1, these oxides have much higher resistivity than the bulk material. Thus the surface layers discharge at a drastically slower rate effectively trapping charges in place.

Material	Resistivity, ρ (nΩ m)
Copper (Cu)	16.8
Copper Oxide (CuO)	$10^9 - 10^{10}$
Aluminum (Al)	28.2
Aluminum Oxide (Al_2O_3)	$10^{19} - 10^{25}$
Titanium (Ti)	420
Titanium Oxide (TiO_2)	$10^{20} - 10^{24}$
Gold (Au)	22.1

Table 4.1: Table of resistivity for a selection of typical materials at room temperature (20°) [11, 12, 13, 14, 15].

The common method to alleviate this effect is to coat the pieces in gold. Gold is a special metal because it does not interact with either air or water. This property is what has attracted humans to gold for millennia and allows archaeologist to find gold artifacts that are in nearly the exact condition as when they were made. Gold is also a good conductor and readily available (albeit at a steep price). If a piece is coated in a thin layer of gold, then the outer most surface will form an equipotential surface which is typically attached to ground. Even if there's a layer of insulator (oxides) underneath the gold layer

with charges stuck in it, charges within the gold will redistribute to maintain zero electric potential, and thus a net zero charge.

Gold-coating the pendulum and any close by surface substantially decreases the electrostatic interactions. However, impurities with the gold layer can cause higher order effects. Impurities in the gold can cause patches of the gold to be at slightly different potential as the rest of the layer. The effect of these patch-charges is only apparent at distances at the same scale as the size of the patches. At large distances, small spatial variations of the potential are washed out since more of the pendulum is in view. Experiments where surfaces must be close-by (e.g. short-range tests of gravity) patch-charge interactions can cause excess coupling and thus noise in the instrument.

4.5 Magnetic Interactions

For the same reason that electrostatic coupling is a worry (10^{40} is a large number), experimenter's must also carefully manage magnetic interactions. The lowest order magnetic interaction between a pendulum and the environment follows:

$$\vec{\tau}_{\text{mag}} = \vec{\mu} \times \vec{B} \tag{4.4}$$

where $\vec{\tau}_{\text{mag}}$ is the torque on the pendulum from the magnetic interaction, $\vec{\mu}$ is the pendulum's magnetic dipole moment, and $\vec{B}$ is the external magnetic field. There are two ways to decrease this interaction: decrease the external magnetic field and decrease the magnetic dipole moment of the pendulum.

The zeroth-order method of minimizing the external magnetic field is to remove any permanent magnetics from the apparatus or located nearby. Once that's complete, the largest magnetic field in most lab settings is that from the Earth's core. The magnitude of the Earth's magnetic field ranges between 25-65 μT depending on geographic location [16] and can vary by up to 25 nT per day and $\sim$1 nT on the few seconds time scale. [17]

4.6 Temperature Variations

4.7 Gas Damping

4.8 Gravity Gradients

Chapter 5

Data Analysis Techniques

5.1 Fourier Analysis

Fourier analysis is the workhorse analysis technique for torsion balance experiments. It consists of breaking the time series of some data into an infinite sum of sinusoidal functions. Typically, the signal of interest for torsion balances is modulated either naturally (e.g. Earth's rotation) or by the experimenter. Thus the analysis for many experiments boils down to extracting the amplitude of a sinusoidal signal. Additionally, the frequency dependent noise of an instrument is the common figure-of-merit when assessing the performance of an apparatus. These make Fourier analysis an unparalleled tool for torsion balance experimentalists.

Let's say we have a data stream of measurements from an apparatus, $x(t)$, and we want to know the frequency content of the data. To evaluate this at all frequencies we would take the Fourier Transform (FT):

$$\tilde{x}(\omega) = \int_{-\infty}^{\infty} x(t) e^{-i\omega t} dt \tag{5.1}$$

where $\tilde{x}(\omega)$ is the Fourier amplitude and $\omega = 2\pi f$ is the angular frequency. The Fourier amplitude is a complex number which gives the amplitude and phase of the sinusoidal component of the data at ω. This becomes clear if we expand the exponential in Equation 5.5 using Euler's formula:

$$\tilde{x}_R(\omega) + i\tilde{x}_I(\omega) = \int_{-\infty}^{\infty} x(t)\cos(\omega t)dt - i\int_{-\infty}^{\infty} x(t)\sin(\omega t)dt \tag{5.2}$$

where $\tilde{x}_R(\omega)$ and $\tilde{x}_I(\omega)$ are respectively the real and imaginary parts of $\tilde{x}(\omega)$. Thus the real part of $\tilde{x}(\omega)$ represents the cosine amplitude while the imaginary part represents the sine amplitude. These can be transformed into amplitude and phase, φ, using:

$$|\tilde{x}(\omega)| = \sqrt{\tilde{x}_R(\omega)^2 + \tilde{x}_I(\omega)^2} \tag{5.3}$$

$$\varphi_x(\omega) = \arctan\left(\frac{\tilde{x}_I(\omega)}{\tilde{x}_R(\omega)}\right) \tag{5.4}$$

To transform back to the time series we can take the Inverse Fourier Transform (IFT):

$$x(t) = \frac{1}{2\pi}\int_{-\infty}^{\infty} \tilde{x}(\omega)e^{i\omega t}d\omega \tag{5.5}$$

Unfortunately, the continuous Fourier transform can not accurately be applied to a real world data set. Data sets are not continuous functions but are instead discrete vectors of measurements recorded at regular intervals. Whereas before we had a continuous function, $x(t)$, really we must analyze a discrete set, $x(t_j)$, of length N. Here $t_j = [0, 1, ..., N-1]/f_s$ is the vector of times corresponding to each data point with f_s being the sampling frequency. With discrete data we can use the Discrete Fourier Transform (DFT):

$$\tilde{x}(\omega_n) = \sum_{j=0}^{N-1} x(t_j)e^{-i\omega_n t_j} \tag{5.6}$$

where $\omega_n = 2\pi f_s/N \times [1, ..., N]$. This has the same interpretation as the Fourier transform, $\tilde{x}(\omega_n)$ represents the cosine and sine amplitudes with frequency ω_n, but now we are restricted to a discrete set of frequencies.

Notice that we can only extract Fourier amplitudes for frequencies between f_s/N and f_s at steps of f_s/N. This has major implications for choosing the amount of time to run an experiment and the rate at which data is taken. Since the highest frequency one can extract is at f_s, the experimenter must ensure that the sampling frequency is well above the frequency of interest. Additionally, f_s/N is equivalent to the the total time span of the data so the apparatus must take data long enough to ensure that f_s/N is lower than the frequency of interest. Both of these situations make intuitive sense. For example, if an experiment is trying to measure a signal that oscillates once per day then it must take data for at least a day in order to see it. Additionally, if the data is only taken once a day then the apparatus would not be able to sense the difference throughout the day.

One significant downside of the discrete Fourier transform is that the amplitude is dependent on the number of data points that are used (i.e. the bin width f_s/N). Thus measurements of different lengths yield different resulting spectra. This confuses the interpretation of spectra if comparing data sets of different size. These issues are alleviated by analyzing the Power Spectral Density (PSD):

$$PSD(\omega_n) = \frac{1}{Nf_s}\left|\sum_{j=0}^{N-1} x(t_j)e^{-i\omega_n t_j}\right|^2 \tag{5.7}$$

The Power Spectral Density is normalized by the length of the data and the sampling frequency to yield measurements that are independent of the length of data and the sampling frequency. This allows us to directly compare results

from different data sets and even different instruments. Also note that the PSD is always real valued instead the complex. This normalization comes with a change in units. While the DFT is in the native units of the data stream, the PSD will be in native units squared over frequency. For example, if $x(t_j)$ is in meters then $\tilde{x}(\omega_n)$ will also be in meters while the PSD will be in meters^2/Hz. To get closer to the native units, we can analyze the Amplitude Spectral Density (ASD):

$$ASD(\omega_n) = \sqrt{\frac{1}{Nf_s}\left|\sum_{j=0}^{N-1} x(t_j)e^{-i\omega_n t_j}\right|^2} \tag{5.8}$$

Note that the DFT, PSD, and the ASD are all related ($PSD = 1/(Nf_s)|DFT|^2$ and $ASD = \sqrt{PSD}$) and contain the same information. The primary difference is the ease of interpretation with the PSD and ASD. Although the normalization of the PSD takes out the dependence on the sampling frequency and number of data points, the measurement of the amplitude of coherent signals with all three methods depends on the number of periods. The amplitude of coherent signals will grow as $\sqrt{\text{number of periods}}$ while incoherent signals will not change.

Let's look at an example data series to see how to analyze the spectra that comes out of these analysis techniques. We will focus on analyzing the ASD as it is the most common spectrum type used for torsion balance experiments. If we have a data stream of distance measurement that has the following form:

$$x(t_j) = a\sin(\omega_0 t_j) + bn_j \tag{5.9}$$

where a and ω_0 are the amplitude and angular frequency of the sinusoidal (coherent) signal, b is the noise amplitude, and n_j is is the incoherent noise as shown in Figure 5.1.

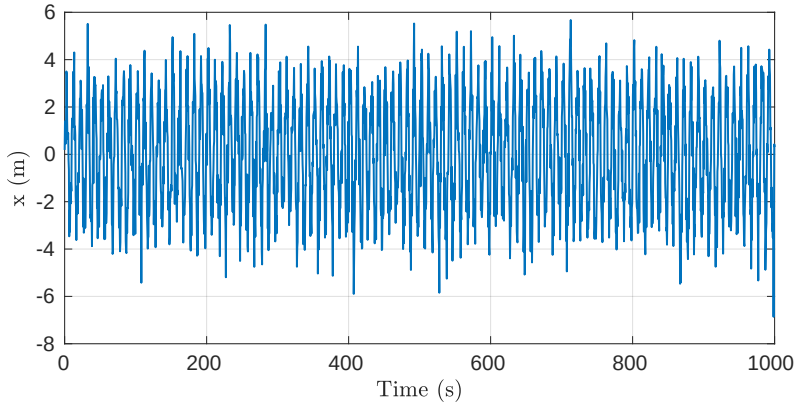

Figure 5.1: Time series of example distance measurements with $a = 3$ m, $b = 1$ m, and $\omega_0 = 2\pi$ (0.1 Hz).

The corresponding Amplitude Spectral Density is shown in Figure 5.2. The spectrum shown a white (frequency independent) noise spectrum and a spike at $f = 0.1$ Hz. The amplitude of the noise in the spectrum is directly $b = 1$ m while the amplitude of the spike which corresponds to the sinusoidal signal is different from the input parameter ($a = 3$ m). However, if we did not know the form of the signal then we could use the spectrum to tell us that it is the sum of a frequency independent noise plus a sinusoidal signal at 0.1 Hz.

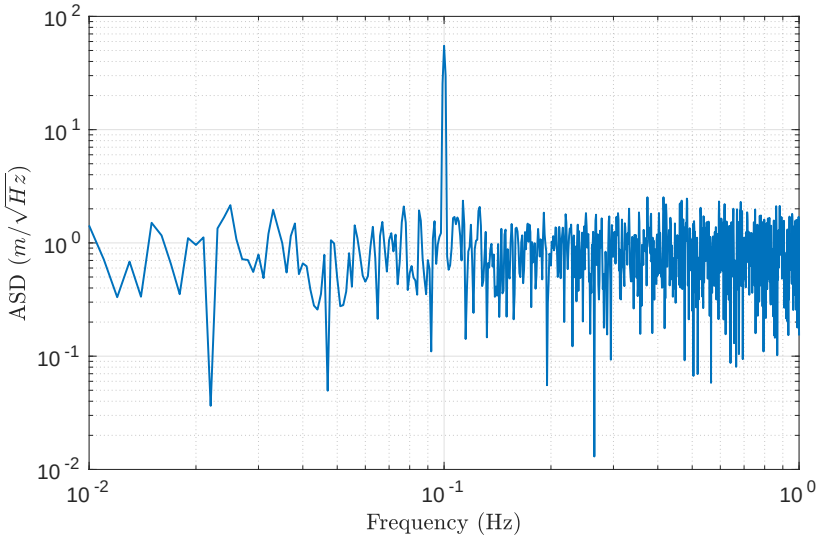

Figure 5.2: Amplitude spectral density of example distance measurements with $a = 3$ m, $b = 1$ m, and $\omega_0 = 2\pi$ (0.1 Hz).

Realistic spectra can be significantly more complicated than the one analyzed here. There can be many sinusoidal signals, frequency dependent (pink) noise, or large semi-coherent bumps. What the spectrum allows the experimenter to separate out all of the structures that make up the signal where as the time series would be essentially uninterpretable. An experienced experimenter can guess at the nature of the various spectral structure to allow an in-depth understanding of a given apparatus with a single plot.

5.2 Linear Least-Squares Fitting

Although Fourier analysis is often used to analyze the data from an apparatus, extracting accurate measurements from a spectrum can be troublesome. The amplitudes pulled off a spectrum must be corrected for a handful of effects in order to yield accurate results. This alleviated by deploying linear least-squares fitting.

Whenever an experimenter goes about fitting data, they are minimizing some sort of error function. There are many choices from depending on the application but the one widely used in torsion balance experiments is the least-squares. Let's say we want to fit data set, $y(t_i)$, that is n-points long to the linear combination of m functions, $f(t_i)_m$. The fit approximation the data set would be:

$$\hat{y}(t_i) = \sum_m a_m f_m(t_i) \tag{5.10}$$

where $\hat{y}$ is the fit approximation of the data and a_m are the weights. To make the mathematics easier, we can vectorize Equation 5.10 by defining the following:

$$\vec{y} = [y(t_1)\ y(t_1)\ ...\ y(t_n)] \tag{5.11}$$
$$\vec{w} = [a_1\ a_2\ ...\ a_m] \tag{5.12}$$
$$\mathbf{X} = [f_1(t_i)\ f_2(t_i)\ ...\ f_m(t_i)] \tag{5.13}$$
$$\hat{\vec{y}} = \vec{w}\ \mathbf{X} \tag{5.14}$$

Notice that $\vec{y}$ is a $1 \times n$ vector, $\vec{w}$ is a $1 \times m$ vector, and $\mathbf{X}$ is a $m \times n$ matrix.

A good fit is defined as the fit that minimizes the least-squares error:

$$\epsilon = \left(\vec{y} - \hat{\vec{y}}\right)^2 = \left(\vec{y} - \vec{w}\ \mathbf{X}\right)^2 \tag{5.15}$$

Once we choose the functions that we want to fit to the only parameter that can vary in Equation 5.15 is $\vec{w}$. Thus to find the fit that minimizes the least-squares error we can differentiate Equation 5.15 with respect to $\vec{w}$ and setting it to zero. Then solving for $\vec{w}$ simplifies to the following:

$$\vec{w} = \left(\mathbf{X}^T\mathbf{X}\right)^{-1}\ \mathbf{X}^T\vec{y} \tag{5.16}$$

Equation 5.16 shows that using linear least-squares fitting is as simple as constructing the correct matrices and then multiplying them together. This has two primary benefits: the calculation is very fast on a computer and, for a given set of data and functions, the solution to linear least-squares fitting is always the same. This is in contrast to non-linear fitting algorithms which numerically minimize an error function which is both computationally intensive and never leads the exact same answer.

Bibliography

[1] Russell Charles Hibbeler. *Mechanics of materials*. Upper Saddle River New Jersey: Prentice Hall, 2003.

[2] Engineering ToolBox. Modulus of rigidity, 2005.

[3] Wikipedia. Fused quartz.

[4] Wikipedia. Yield.

[5] Engineers Edge. Yield strength.

[6] AZo Materials. Beryllium copper.

[7] C. A. Hagedorn, S. Schlamminger, and J. H. Gundlach. Quality factors of bare and metal-coated quartz and fused silica torsion fibers. *AIP Conference Proceedings*, 873(1):189–193, 2006.

[8] Herbert B. Callen and Theodore A. Welton. Irreversibility and generalized noise. *Phys. Rev.*, 83:34–40, Jul 1951.

[9] Peter R. Saulson. Thermal noise in mechanical experiments. *Phys. Rev. D*, 42:2437–2445, Oct 1990.

[10] Michael P Ross. *Precision Mechanical Rotation Sensors for Terrestrial Gravitational Wave Observatories*. PhD thesis, University of Washington, 2020.

[11] R. A. Matula. Electrical resistivity of copper, gold, palladium, and silver. *Journal of Physical and Chemical Reference Data*, 8(4):1147–1298, 1979.

[12] Raymond A Serway and John W Jewett. *Principles of physics*, volume 1. Saunders College Pub. Fort Worth, TX, 1998.

[13] Wikipedia. Electrical resistivity and conductivity.

[14] AZo Materials. Titanium dioxide.

[15] Paul G Slade. *Electrical contacts: principles and applications*. CRC press, 2017.

[16] C. C. Finlay, S. Maus, C. D. Beggan, T. N. Bondar, A. Chambodut, T. A. Chernova, A. Chulliat, V. P. Golovkov, B. Hamilton, M. Hamoudi, R. Holme, G. Hulot, W. Kuang, B. Langlais, V. Lesur, F. J. Lowes, H. Lühr, S. Macmillan, M. Mandea, S. McLean, C. Manoj, M. Menvielle, I. Michaelis, N. Olsen, J. Rauberg, M. Rother, T. J. Sabaka, A. Tangborn, L. Tøffner-Clausen, E. Thébault, A. W. P. Thomson, I. Wardinski, Z. Wei, and T. I. Zvereva. International Geomagnetic Reference Field: the eleventh generation. *Geophysical Journal International*, 183(3):1216–1230, 12 2010.

[17] Janez Stepi et al. Spectroscopy: Nmr down to earth. *Nature*, 439(7078):799–802, 2006.